FULL PAPER

BJC

British Journal of Cancer (2013) 109, 2131–2141 | doi: 10.1038/bjc.2013.537

Keywords: prostate cancer; chemotherapeutic; toluidine sulphonamide; taxane; MDR1 drug resistance; Hif1

The novel toluidine sulphonamide EL102 shows pre-clinical *in vitro* and *in vivo* activity against prostate cancer and circumvents MDR1 resistance

A P Toner[1], F McLaughlin[2], F J Giles[1,3], F J Sullivan[1,3,4], E O'Connell[5], L A Carleton[6], L Breen[7], G Dunne[7], A M Gorman[6], J D Lewis[2] and S A Glynn*[,1]

[1]*Prostate Cancer Institute, National University of Ireland Galway, Galway, Ireland;* [2]*Elara Pharmaceuticals GmbH, Heidelberg, Germany;* [3]*HRB Clinical Research Facilities Galway & Dublin, National University of Ireland Galway and Trinity College, Dublin, Ireland;* [4]*Department of Radiation Oncology, Galway University Hospital, Galway, Ireland;* [5]*National Centre for Biomedical Engineering Science, National University of Ireland Galway, Galway, Ireland;* [6]*Apoptosis Research Centre, School of Natural Sciences, National University of Ireland Galway, Galway, Ireland and* [7]*National Institute for Cellular Biotechnology, Dublin City University, Dublin, Ireland*

Background: Taxanes are routinely used for the treatment of prostate cancer, however the majority of patients eventually develop resistance. We investigated the potential efficacy of EL102, a novel toluidine sulphonamide, in pre-clinical models of prostate cancer.

Methods: The effect of EL102 and/or docetaxel on PC-3, DU145, 22Rv1 and CWR22 prostate cancer cells was assessed using cell viability, cell cycle analysis and PARP cleavage assays. Tubulin polymerisation and immunofluorescence assays were used to assess tubulin dynamics. CWR22 xenograft murine model was used to assess effects on tumour proliferation. Multidrug-resistant lung cancer DLKPA was used to assess EL102 in a MDR1-mediated drug resistance background.

Results: EL102 has *in vitro* activity against prostate cancer, characterised by accumulation in G2/M, induction of apoptosis, inhibition of Hif1α, and inhibition of tubulin polymerisation and decreased microtubule stability. *In vivo*, a combination of EL102 and docetaxel exhibits superior tumour inhibition. The DLKP cell line and multidrug-resistant DLKPA variant (which exhibits 205 to 691-fold greater resistance to docetaxel, paclitaxel, vincristine and doxorubicin) are equally sensitive to EL102.

Conclusion: EL102 shows potential as both a single agent and within combination regimens for the treatment of prostate cancer, particularly in the chemoresistance setting.

Prostate cancer is the second most common cancer diagnosed in men globally, accounting for 13.6% of all cancer cases in men worldwide (http://globocan.iarc.fr) in 2008. In the United States, the National Cancer Institute (NCI) estimates that 241 740 men will have been diagnosed with and 28 170 men will have died of cancer of the prostate during 2012 (http://seer.cancer.gov). Several choices exist for the treatment of early prostate cancer, including radical prostatectomy, external beam radiation and prostate brachytherapy, with similar outcomes (Peinemann *et al*, 2011). Despite advances in primary treatment of prostate cancer, in a subset of patients the disease progresses and distant metastases develop. While these patients can initially be treated with androgen

*Correspondence: Dr S Glynn; E-mail: sharon.glynn@nuigalway.ie

Received 17 May 2013; revised 13 August 2013; accepted 14 August 2013; published online 19 September 2013

ablation therapies, eventually their cancer will become refractory and they will succumb to their illness. In the mid-2000s, introduction of taxane-based therapies improved the outcomes of patients with metastatic castrate-resistant prostate cancer, extending survival by several months. The taxane family, which includes paclitaxel, docetaxel and the newly approved cabazitaxel are natural or semi-synthetic plant derivatives that are widely used in the treatment of metastatic castrate-resistant prostate cancer (mCRPC). Their mechanisms of action have been widely reported (Rowinsky *et al*, 1990; Jackson *et al*, 2007) and have been shown to act as mitotic arresting agents (Wani *et al*, 1971; Douros and Suffness, 1981). The dynamic ability of a cell to assemble and disassemble the architecture of the microtubules from and to tubulin components, respectively, is curtailed greatly by the introduction of taxanes (Manfredi and Horwitz, 1984). Phase III trials demonstrated that docetaxel–estramustine combinations conferred median survival advantage of ~3 months compared with the standard mitoxantrone–prednisone combination (Petrylak *et al*, 2004; Berthold *et al*, 2008). Since 2010, an additional six drugs have been approved for use in patients with metastatic castrate-resistant prostate cancer. These include drugs targeting androgen receptor activity (abiraterone acetate and enzalutamide), drugs targeting bone metastasis and the micro-enviroment (denosumab and alpharadin), immunotherapeutics (Sipuleucel-T) and new taxanes (cabazitaxel) (Heidegger *et al*, 2013).

It is postulated that combination treatments of docetaxel with alternative cytotoxics could prevent this late-stage resistance, with such other compounds acting in an additive or synergistic fashion. While phase II trials with various combinations of new drugs have suggested promise for emerging docetaxel combination therapies (Oh *et al*, 2003; Ferrero *et al*, 2006; Tester *et al*, 2006; Kikuno *et al*, 2007; Garcia *et al*, 2011), of note is the fact that no drug has yet been shown to provide survival benefit when combined with docetaxel in phase III trials (Antonarakis and Eisenberger, 2013). This suggests that there is a need to identify novel compounds for efficacy as single agents or for use in combination with taxane-based therapies.

Here, we present preliminary data on the efficacy of a novel toluidine sulphonamide, EL102, *in vitro* against prostate cancer cell lines and in an *in vivo* prostate cancer xenograft mouse model, demonstrating EL102's ability to work in combination with docetaxel, and circumvent multiple drug resistance mediated by P-glycoprotein (Pgp). EL102 was identified by Elara Pharmaceuticals as a potential chemotherapeutic agent during a screen of novel small molecule inhibitors using the NCI-60 cell line panel assessing for growth inhibition potential. EL102 is a later generation derivative of the family of toluidine sulphonamide hypoxia-induced factor 1 (Hif1α) inhibitors described by (Wendt *et al*, 2011). This is the first report on the biological actions of EL102 on cancer cells, focusing on its use as an anti-prostate cancer chemotherapeutic.

MATERIALS AND METHODS

Ethics statement. Tumour xenograft models were performed at EPO Experimental Pharmacology and Oncology Berlin-Buch GMBH, Germany. These studies were performed under the approval A0452/08 (Landesamt für Gesundheit und Sozaiales, Berlin). The study was performed according to the German Animal Protection Law and the UICCR (2010).

Chemicals. The compound EL102 was developed and supplied by Elara Pharmaceuticals GmbH (Heidelberg, Germany). Docetaxel was purchased from Sigma-Aldrich (Dublin, Ireland; #01885-5MG-F). Unless otherwise stated, all chemicals were obtained from Sigma-Aldrich.

Cell lines. DU145, PC-3, 22Rv1 and CWR22 were sourced from the American Type Culture Collection (ATCC) (Manassas, VA, USA) and cultured according to recommendations. In brief, CWR22 and 22Rv1 were cultured in RPMI 1640 medium with L-glutamine (Sigma, #R8758), and supplemented with 10% fetal bovine serum (FBS) (Sigma, #F7524). DU145 was cultured in Minimum Essential Medium (1 ×) with Earles (Gibco, Bio-Sciences, Dun Laoghaire, Ireland; #22561-021) supplemented with 10% FBS. PC-3 was cultured in F12 Nutrient Mixture (HAM) medium, with L-glutamine (Gibco #21765-029) supplemented with 10% FBS. Non-small cell lung carcinoma, DLKP and its doxorubicin-selected variant DLKPA (Pgp-mediated resistance) was developed by the National Institute for Cellular Biotechnology (Dublin City University, Dublin, Ireland) and maintained in DMEM/Hams F12 (1 : 1) supplemented with 5% FBS and 1% L-glutamine. With the exception of RPMI 1640 and FBS (Sigma), all media and supplements were Gibco (Life Technologies), purchased from Bio-Sciences. All media contained 1% of (100 ×) antibiotic-antimycotic (Life Technologies) with the exception of DLKP and DLKPA.

Prostate cancer cell line toxicity assays. Sulforhodamine B (SRB)-based assays were used to assess the effects of docetaxel and EL102 administration on cell viability as previously described (Vichai and Kirtikara, 2006). In brief, the relevant amounts of docetaxel or EL102, or combinations of both were preloaded into a 96-well plate (Sarstedt, Ireland) using the Perkin Elmer Janus Automated Workstation. Cells were trypsinised, counted and dispensed by the robotics into a 96-well cell culture plate, at a cell density of 1.9×10^4 cells per well. The drugs were then transferred by the robotics from the drug plate to the 96-well cell culture plate. This was left in culture for 72 h at 37 °C in a 5% CO_2 incubator. Separately, three rows of a non-drug-treated 96-well plate were seeded with the same cell density. After 2–4 h incubation at 37 °C, 5% CO_2, to allow for attachment of cells, 100 μl of fixative (cold 10% trichloroacetic acid (TCA) (Sigma, #T0699)) was added to the wells and left to incubate at 4 °C for 30 min. Wells were then submerged in distilled water and tapped dry four times, to ensure complete removal of TCA. The plate was left to air dry. This plate served as day 0 plate. The 72-h incubated drug-treated plates were fixed in the same way. All plates were subsequently stained with 0.057% SRB solution in 1% acetic acid for 30 min and washed four times with 1% acetic acid, to remove excess stain. These were allowed to air dry. Stain was eluted by addition of 10 mM Tris base solution to the wells followed by 30 min incubation. Plates were read at 531 nm using a Victor X5 Multilabel plate reader. Mean optical density values of Day 0 plates were subtracted from those of sample plates. A percentage viability curve was calculated based on these values and the IC_{50} was determined. Error was presented at ± the percentage coefficient variant (%CV). All cytotoxicity assays were conducted in triplicate.

Multidrug-resistant cell line toxicity assays. Cells were trypsinised and resuspended in fresh media at 2×10^4 cells per ml. A volume of 100 μl of cell suspension was seeded into each well of a 96-well plate and cultured overnight in 5% CO_2 at 37 °C. Varying concentrations of EL102 or docetaxel were added in replicate ($n = 8$) and incubated at 37 °C for a further 72 h. After this incubation, media were removed from each well, which was then washed twice with 100 μl Dulbecco's phosphate buffered saline (dPBS). Having aspirated the last of the dPBS, 100 μl of freshly prepared phosphatase substrate (10 mM *p*-nitrophenol phosphate in 0.1 M sodium acetate (Sigma, #N7653-100ML), 0.1% Triton X-100 (Merck, Darmstadt, Germany; pH 5.5) was added to each well (Martin and Clynes, 1991). Plates were incubated in the dark at 37 °C for 2 h. The enzymatic reaction was stopped by the

addition of 50 μl of 1 M NaOH to each well. The plates were read on a dual beam plate reader at 405 nm with a reference wavelength of 620 nm. A percentage viability curve was calculated based on these values and the IC_{50} was determined. Error was presented at ± the percentage coefficient variant (%CV). All cytotoxicity assays were conducted in triplicate.

Sub-G1 and cell cycle analysis by flow cytometry. Cells were seeded at a density of 1.3×10^5 cells per well in a final volume of 2 ml/well in a six-well plate and left to attach overnight at 37 °C in a 5% CO_2 incubator. Cells were treated with 1 ml of medium spiked with appropriate concentrations of EL102, docetaxel or both. Following treatments, plates were returned to the incubator for 24, 48 and 72 h. The medium from each well liquid fraction was transferred to labelled 15 ml tubes. Remaining attached cells were gently washed with 300 μl Hanks' balanced salt solution (Sigma, #H6648) at room temperature. These washings were retained and added to the medium in the appropriate labelled 15-ml tubes. Cells were trypsinised with 750 μl trypsin-EDTA for 5 min at 37 °C. Trypsinisation was stopped by re-addition of 1 ml of medium from the appropriate well of origin. Cell suspensions were combined with the medium in the appropriate 15-ml tubes, and cell pellets were collected by centrifugation at $1000 \times g$ at 4 °C for 5 min using soft acceleration. The supernatant was removed and the cell pellets were placed on ice. Pellets were resuspended in 500 μl ice-cold dPBS (Sigma, #D8537) and transferred to labelled 1.5-ml tubes. Cell pellets were again recovered following centrifugation at 4 °C for 5 min at $1000 \times g$ and supernatant was discarded. Cells were resuspended in 150 μl dPBS. A volume of 350 μl ice-cold 100% ethanol was added dropwise to the cell suspension while vortexing, to avoid clumping. Cells were incubated on ice for 30 min. Following overnight storage at −20°C, cells were then centrifuged at $1000 \times g$ for 5 min using soft acceleration. Each pellet was washed in 500 μl dPBS and suspension was centrifuged at $1000 \times g$ for 5 min using soft acceleration, after which supernatant was removed. Each cell pellet was resuspended in propidium iodide, PI/RNAse staining buffer (BD Pharmingen, BD Biosciences, Oxford, England; #550825). Sample suspensions were incubated in the dark for 15–20 min and measured by flow cytometry on BD FACSCanto II (BD Biosciences), channel PE. Logarithmic and linear regression was performed as needed for $SubG_1$ and cell cycle analyses. Flow cytometric analyses were conducted using Cyflogic software (CyFlo Ltd, Turku, Finland).

Tubulin polymerisation assay. The HST-tubulin polymerization assay kit (Cytoskeleton, Tebu-Bio, Peterborough, UK; #BK004P) was used as per the manufacturer's instructions. In brief, the assay was performed using a 96-well plate. To each well, with the exception of the blank control, 4 mg/ml of tubulin was added. Each well contained a concentration of the drug of interest and G-PEM buffer (80 mM PIPES, pH 6.9; 2 mM $MgCl_2$; 0.5 mM EGTA; 1 mM GTP). Drug concentrations used included 5 μM EL102, 2 μM docetaxel and 5 μM EL102 and 2 μM docetaxel combined. A concentration of 2 μM of nocodazole was used as an inhibitor of tubulin polymerisation control. The 96-well plate was read on a 96-well plate reading spectrophotometer in kinetic mode (61 cycles: 1 s read per well per min) at wavelength 405 nm. Readings were zeroed by the blank control and mean sample values were calculated with error bars ± s.e.m.

Tumour xenograft models. CWR22 tumours were taken from an *in vivo* passage, cut into small fragments and transplanted subcutaneously (s.c.) into the flank of 48 nude mice. At day 13, when the tumours were palpable, mice were randomised into 10 groups with 8 mice each and treatment initiated. The groups included: (A) vehicle (10% DMSO, 10% Cremophor, aqua per os (p.o.), (B) docetaxel 12 mg kg^{-1} intravenously (i.v.), (C) EL102 12 mg kg^{-1} via p.o. (0700 hours and 1700 hours daily), (D) EL102 15 mg kg^{-1} via p.o. (E) docetaxel 12 mg kg^{-1} via i.v. and EL102 12 mg kg^{-1} via p.o. and (F) docetaxel 12 mg kg^{-1} via i.v. and EL102 15 mg kg^{-1} via p.o. The injection volume was 5 ml kg^{-1}. The different tumour groups were sacrificed on separate days for ethical reasons (large tumours). Tumour diameter of the s.c. tumour and mouse body weight were measured twice a week with a caliper. Tumour volumes were calculated according to $V = (\text{length} \times (\text{width})^2/2$. Tumour xenograft models were performed at EPO Experimental Pharmacology and Oncology Berlin-Buch GMBH, Germany. These studies were performed under the approval A0452/08 (Landesamt für Gesundheit und Sozaiales, Berlin). The study was performed according to the German Animal Protection Law and the UICCR, 2010.

Western blot analysis. Cells were seeded in 10-cm^3 dishes at a cell density of 1×10^6 per dish, and treated with the relevant doses of EL102 and docetaxel for the required time period. After treatment, cells were rinsed twice with cold PBS and lysed directly on the dish with cold RIPA buffer (Pierce, Fisher Scientific, Dublin, Ireland; #89900) supplemented with protease inhibitors (Pierce, #78410), scraped, and spun at 14 000 **g** for 15 min at 4 °C. Supernatant was collected and stored at −20 °C for western blot analysis of protein expression. Extracted protein was quantified using a BCA kit (Fisher Scientific, Dublin, Ireland). Both PARP and Hif1α levels were detected through use of primary anti-PARP rabbit polyclonal antibody (Cell Signaling Technology Inc., Danvers, Massachusetts, USA; #9542) and anti-Hif1α rabbit polyclonal antibody (Millipore, Temecula, California, USA; #07-628), respectively. The anti-PARP antibody was diluted 1 : 1000 and anti-Hif1α antibody was diluted 1 : 1500 in 5% skimmed milk reconstituted in 1 × Tris-buffered saline (TBS) (pH 8) 0.1% Tween. These dilutions were added to the transfer membrane, and shaken overnight at 4 °C, following a 1 h RT blocking in 5% skimmed milk in TBS. Mouse monoclonal anti-β-actin antibody (Thermo-Scientific Pierce, Fisher Scientific, Dublin, Ireland; #10624754) was used to confirm even protein loading. Secondary antibodies used were IRDye 800CW goat anti-rabbit IgG (LI-COR Biosciences, Cambridge, UK; #926-32211) and IRDye 680LT goat anti-mouse IgG (LI-COR Biosciences; #926-68020) and detection was imaged on the LI-COR ODYSSEY CLx imaging system.

Immunocytofluorescence. Coverslips, pre-sterilised in 100% ethanol, were inserted to the base of each well of a six-well plate. Cells were seeded at a density of 1×10^6 per well and allowed overnight attachment at 37 °C, in a 5% CO_2 incubator. Cell treatment and fixation was carried out at the relevant time points. Cells were fixed for 10 min in ice-cold methanol. For immunocytofluorescence, primary antibodies against β-tubulin (Abcam, Cambridge, UK #AB6046), diluted 1 : 200, and acetylated tubulin (Sigma, #T6793), diluted 1 : 200, were used with secondary fluorescent conjugates Rhodamine Red-X-AffiniPure Fab Fragment goat anti-mouse IgG (H + L) (Jackson ImmunoResearch Europe Ltd., Suffolk, UK #JAC-115297003), diluted 1 : 50, and Alexa Fluor 647 donkey anti-rabbit IgG (Invitrogen, Bio Sciences, Dun Laoghaire, Ireland; #A31573), diluted 1 : 50, respectively. These cells were counterstained with mounting medium SlowFade Gold antifade reagent (Invitrogen; #S36936) supplemented with 4′,6-diamidino-2-phenylindole dihydrochloride (DAPI) (Sigma; #D8417) diluted 1 : 100 and coverslips were fixed to slides using nail varnish. Staining was imaged using Delta Vision Core Imaging System C0607 (Applied Precision, Issaquah, WA, USA). Image analysis was conducted using SoftWoRx software (Applied Precision) and FIJI software (GPL v2).

Statistics. Data analysis was performed using GraphPad Prism Version 5. All statistical tests were 2-sided, and an association was considered statistically significant with P-values < 0.05. The Student's t-test was used to analyse differences between treatment

groups in cell culture experiments. IC_{50} values were calculated using log (inhibitor) *vs* normalised response curve ($Y = 100/(1 + 10\text{^}(X - \log IC_{50}))$). For the xenograft model, a one-way ANOVA with Tukey's multiple comparisons test was used to determine whether there were significant differences in the tumour volumes or body weights between the treatment groups. Additionally, linear regression was used to fit a slope to the tumour growth curve to determine whether the rate of growth differed between the treatment groups.

RESULTS

EL102 inhibits prostate cancer cell line viability *in vitro*. EL102, whose chemical structure is shown in Figure 1A, is a novel toluidine sulphonamide. To determine whether EL102 could have utility as a chemotherapeutic agent in prostate cancer, we determined the effects of increasing doses of EL102 on prostate cancer cell line viability in comparison to the clinically used docetaxel. A panel of four prostate cancer cell lines were used in this study, including CWR22 (androgen receptor (AR)-positive, androgen dependent, non-metastatic), its daughter cell line 22Rv1 (AR-positive, androgen independent, non-metastatic), PC-3 (AR-negative, derived from metastatic bone lesion) and DU145 (AR-negative, derived from metastatic brain lesion). Figures 1B and C demonstrate the effects of increasing doses of EL102 and docetaxel as single agents, respectively, on prostate cancer cell line viability over a 3-day drug exposure. This demonstrates that while docetaxel is more potent than EL102, both EL102 and docetaxel decrease prostate cancer cell viability in a dose-dependent manner. Table 1 shows that CWR22 and 22Rv1 are equally sensitive to docetaxel (IC_{50} 0.4–0.6 nM), while bone metastatic cell line, PC-3, is 2.5–10 fold more resistant to docetaxel than the other cell lines (IC_{50} 3.8 nM). EL102 inhibited cell proliferation with an IC_{50} of ~21–40 nM. By comparison, bone metastatic PC-3 cells were twofold more resistant than CWR22 and 22Rv1 to EL102, and were equally as sensitive as brain metastatic cell line DU145.

Cell lines with MDR1-mediated drug resistance are sensitive to EL102. A classic method of chemotherapeutic drug resistance involves the overexpression of drug resistance pump Pgp. We tested EL102 in a poorly differentiated squamous lung carcinoma cell line pair: DLKP and its doxorubicin-selected variant DLKPA (Clynes *et al*, 1992). Table 2 shows that DLKPA is cross-resistant to the taxanes, docetaxel (253-fold) and paclitaxel (258-fold). Its

Table 1. Prostate cancer cell line inhibition by docetaxel and EL102

Cell line	Docetaxel (nM) IC_{50} ± s.d.	EL102 (nM) IC_{50} ± s.d.
CWR22	0.4 ± 0.01	24.0 ± 1.41
22Rv1	0.6 ± 0.15	21.7 ± 2.31
DU145	1.5 ± 0.18	40.3 ± 7.71
PC-3	3.8 ± 0.76	37.0 ± 2.00

Abbreviation: s.d. = standard deviation.

Table 2. Cross-resistance profile of DLKP and DLKPA

	DLKP IC_{50} ± s.d.	DLKPA IC_{50} ± s.d.	Fold change
Adriamycin (nM)	24 ± 2	4900 ± 300	204
Docetaxel (nM)	0.15 ± 0.04	38 ± 3.0	253
Paclitaxel (nM)	1.2 ± 0.5	310 ± 25	258
EL102 (nM)	14.4 ± 0.8	16.3 ± 1.2	1.1
Vincristine (nM)	0.91 ± 0.1	629 ± 160	691

Abbreviation: s.d. = standard deviation.

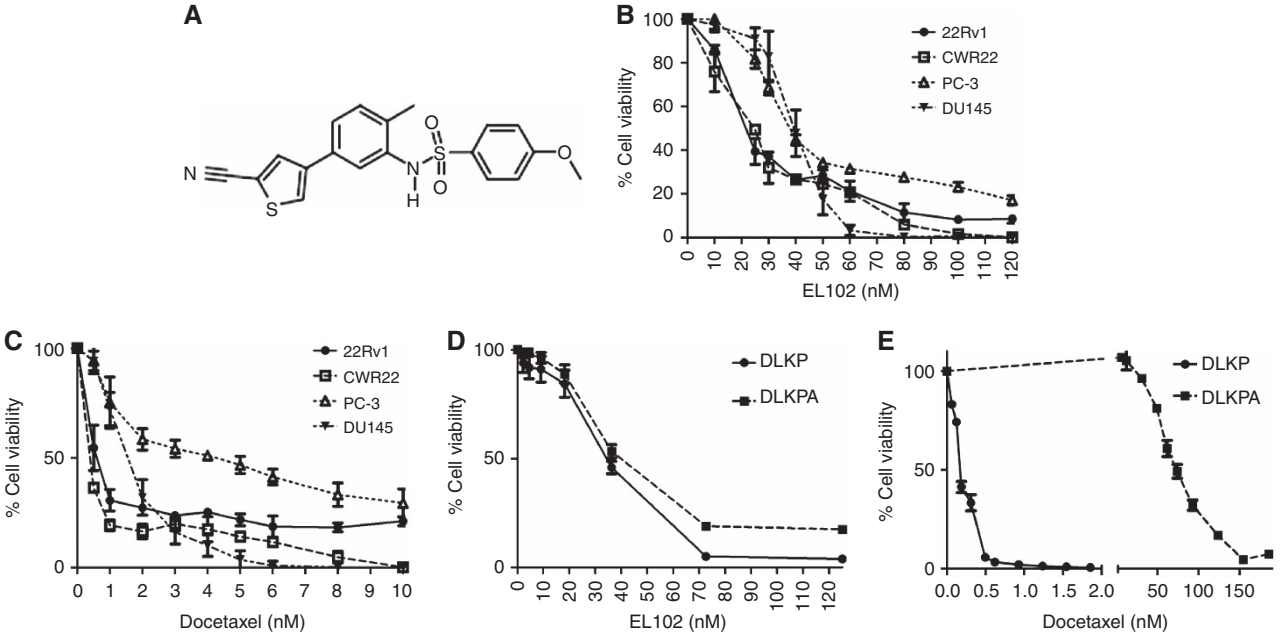

Figure 1. Impact of EL102 and docetaxel on prostate cancer cell line viability *in vitro*. (**A**) Chemical structure of EL102. (**B**) Dose response effects of EL102 on prostate cancer cell line viability over 72-h exposure. (**C**) Dose response effects of docetaxel on prostate cancer cell line viability over 72-h exposure. (**D**) Effect of EL102 on doxorubicin and docetaxel-resistant DLKPA lung cancer cell line viability *vs* DLKP parental lung cancer cell line. (**E**) Comparison of docetaxel sensitivity in the doxorubicin and docetaxel-resistant DLKPA lung cancer cell line viability *vs* DLKP parental lung cancer cell line.

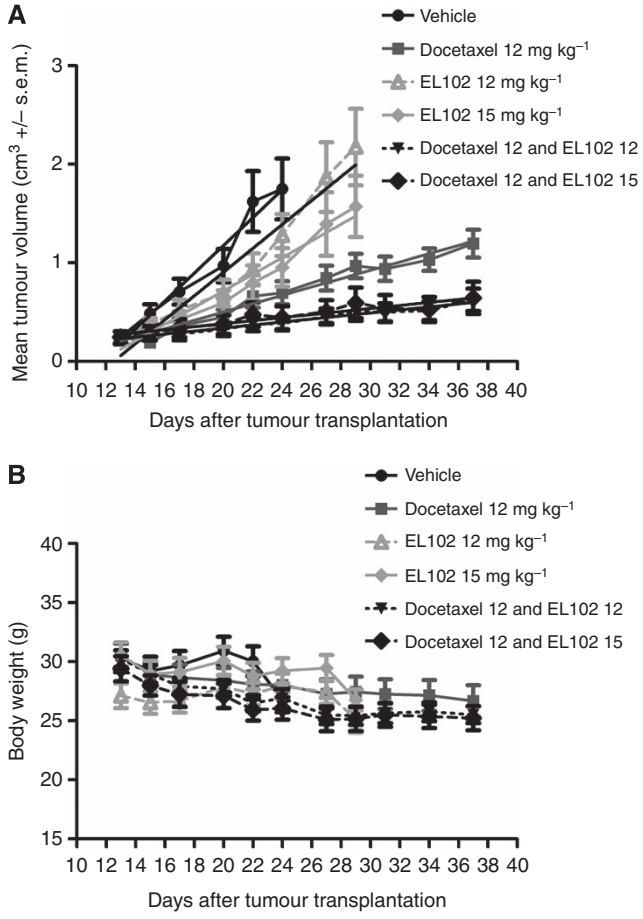

Figure 2. Impact of EL102 and docetaxel alone and in combination on CWR22 xenograft tumour volume. (**A**) Effect of vehicle *vs* 12 mg kg^{-1} docetaxel, *vs* 12 mg kg^{-1} EL102, *vs* 15 mg kg^{-1} EL102, *vs* 12 mg kg^{-1} docetaxel plus 12 mg kg^{-1} EL102, *vs* 12 mg kg^{-1} docetaxel plus 15 mg kg^{-1} EL102, on CWR22 tumour volume using a 5-day on/2-day off schedule (tumour volume (cm^3) ± s.e.m.). (See Supplementary Table 1 for one-way ANOVA comparing tumour volume at each time point). (**B**) Effect of vehicle *vs* 12 mg kg^{-1} docetaxel, *vs* 12 mg kg^{-1} EL102, *vs* 15 mg kg^{-1} EL102, *vs* 12 mg kg^{-1} docetaxel plus 12 mg kg^{-1} EL102, *vs* 12 mg kg^{-1} docetaxel plus 15 mg kg^{-1} EL102, on mouse body weight (Note: vehicle group killed on day 24 due to tumour size). (See Supplementary Table 2 for one-way ANOVA comparing body weight at each time point.)

mechanism of resistance is primarily through overexpression of Pgp as previously described (Keenan *et al*, 2009; Collins *et al*, 2010; Dunne *et al*, 2011). While DLKPA overexpresses Pgp, it does not express the MRP1 or BCRP drug resistance pumps (Collins *et al*, 2010). Figure 1D and Table 2 shows that while the DLKPA variant is resistant to docetaxel, both parent cell line DLKP and its drug-resistant variant DLKPA are equally sensitive to EL102 (Figure 1E).

EL102 potentiates the effects of docetaxel *in vivo*. To determine whether EL102 could be used in combination with docetaxel *in vivo*, we examined the ability of the combination of docetaxel with EL102 to inhibit tumour growth in a CWR22 xenograft mouse model (Figure 2A). While administration of 12 mg kg^{-1} EL102 using a 5-day on/2-day off regimen did not significantly inhibit rate of tumour growth compared with vehicle (slope (R^2): vehicle 0.1414 ± 0.01438 (0.9603) *vs* EL102 12 mg kg^{-1}, 0.1210 ± 0.01179 (0.9462), *F*-test: $P = 0.3385$), increasing the dosage to 15 mg kg^{-1} EL102 did inhibit the rate of tumour growth compared with vehicle (slope (R^2): vehicle 0.1414 ± 0.01438 (0.9603) *vs* EL102 15 mg kg^{-1}, 0.08451 ± 0.006934 (0.9612), *F*-test: $P = 0.003$). Administration of 12 mg kg^{-1} docetaxel decreased the rate of tumour growth more efficiently than EL102 (slope (R^2): vehicle 0.1414 ± 0.01438 (0.9603) *vs* docetaxel 12 mg kg^{-1} 0.04230 ± 0.002531 (0.9688), *F*-test: $P < 0.0001$), while the combination of both drugs had the largest effect on inhibition of tumour growth, suggesting that these drugs work well together in combination *in vivo* (slope (R^2): vehicle 0.1414 ± 0.01438 (0.9603) *vs* docetaxel 12 mg kg^{-1} and EL 102 12 mg kg^{-1} 0.01533 ± 0.0008838 (0.9709), *F*-test: $P < 0.0001$ or vehicle, 0.1414 ± 0.01438 (0.9603) *vs* docetaxel 12 mg kg^{-1} and EL 102 15 mg kg^{-1}, 0.01537 ± 0.001704 (0.9003), *F*-test: $P < 0.0001$). Comparison of the docetaxel arm *vs* the combination arms showed a significant difference in the rate of tumour growth indicating that the addition of EL102 to docetaxel improves anti-tumour activity (*F*-test, $P < 0.0001$). Supplementary Table 1 describes the results of a one-way ANOVA test on this model, using a Tukey's *post-hoc* test to assess statistical difference in tumour volume between the treatment arms at different time points. Additionally to determine if combining EL102 and docetaxel was well tolerated by the mice with minimal adverse effects, we compared changes in mean body weight between the treatment arms and found no significant differences between the groups compared with vehicle or between different treatment arms (Figure 2B). Supplementary Table 2 describes the results of a one-way ANOVA test on this model, using a Tukey's *post-hoc* test to assess statistical difference in body weights between the treatment arms at different time points.

EL102 is cytotoxic to prostate cancer cell lines and induces cellular apoptosis. As demonstrated in Figure 1B and Table 1, EL102 is a potent inhibitor of prostate cancer cell viability, and when combined with docetaxel *in vivo* inhibits tumour growth to a greater extent than either alone (Figure 2A). In an attempt to further address the mechanisms driving the combination of the two agents we performed an *in vitro* combination assay looking at the impact of the combining EL102 and docetaxel on cell viability (Figure 3). Results show that *in vitro,* combining EL102 and docetaxel does not have an additive effect on inhibition of cell viability. To determine whether these effects were cytostatic or cytotoxic, we quantified the number of cells in subG$_1$ phase indicating loss of cellular DNA and entry into late apoptosis using logarithmic scale propidium iodide flow cytometry (Figure 4). Cells were exposed to increasing doses of EL102 and docetaxel. EL102 was an equally strong inducer of apoptosis at 100 nM in all four prostate cancer cell lines, while it failed to induce apoptosis at 10 nM of EL102 (Figure 4A–D), despite inhibiting cell viability by approximately 25–30% at 10 nM (Figures 3A–D). Apoptosis was detectable at 24 h and steadily increased over the next 48 h (72 h total), indicating that EL102-dependent inhibition of cell viability is partially due to cytotoxic effects, namely induction of apoptosis. Similarly, docetaxel induced apoptosis in all 4 cell lines in a dose-dependent and temporal manner. When EL102 and docetaxel were administered in combination *in vitro*, no additive effects were seen on the levels of apoptosis in these cell lines (Figure 4), similar to the cell viability assays (Figure 3). Of note though is that while 10 nM of EL102 failed to induce increased apoptosis (Figure 4), it did lead to significantly decreased % cell viability compared to control (Figure 3) in each cell line, indicating non-apoptosis effects at low concentrations. Figures 5A–D shows representative histograms from these experiments in the DU145 prostate cancer cell line. In addition to demonstrating an increase in subG1 accumulation, the histograms indicated that combining the agents altered the cell cycle dynamics. These effects in DU145 are quantified at 24 (Figure 5E), 48 (Figure 5F) and 72 (Figure 5G) h, and demonstrate that combining EL102 and docetaxel causes greater loss of cells from G$_1$ and accumulation in G$_2$/M than either alone by 24 h at low doses. Also of interest in the combination assays cell profile images is a peak beyond the G$_2$/M peak which

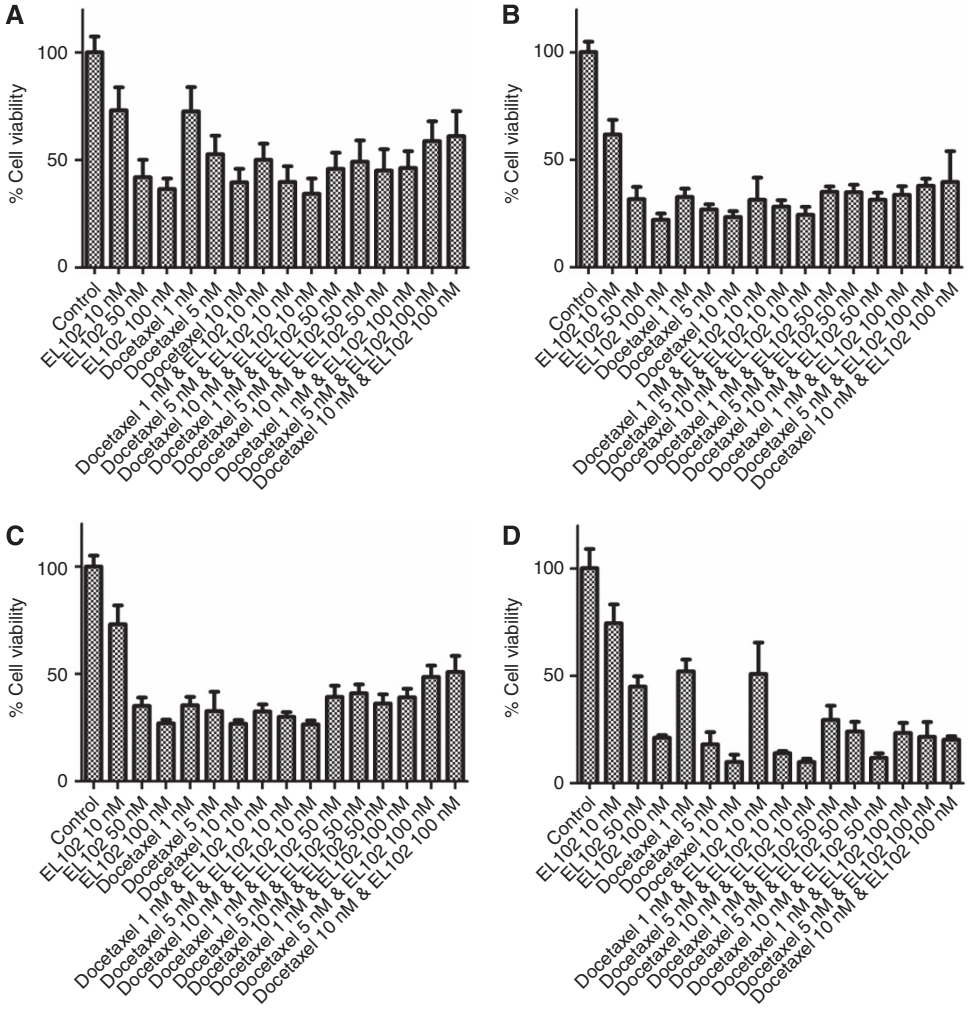

Figure 3. Impact of EL102 and docetaxel combination treatment on prostate cancer cell line viability *in vitro*. Effect of EL102 and docetaxel in combination of *in vitro* cell viability after 72 h in (**A**) CWR22, (**B**) 22Rv1, (**C**) PC-3 and (**D**) DU145 prostate cancer cell. (See Supplementary Table 3 for results of one-way ANOVA comparing cell viability between each treatment.)

represents a subset of cells with increased DNA content (8X). Apoptosis induction upon *in vitro* EL102 and docetaxel administration was further evidenced by detection of PARP cleavage in protein extracted from DU145 cell lysate, 24 and 48 h post-treatment. PARP cleavage increases in a dose-dependent manner and over time with the strongest detection seen in lysates of cells cultured with dual treatments at 48 h (Figure 4E).

EL102 has both cytostatic and cytotoxic effects. Figure 5 indicated that EL102 may cause accumulation of cells in G_2/M. To further quantify the accumulation of cells in the various phases of the cell cycle after exposure to EL102 we performed linear scale propidium iodide flow cytometry. Figure 5 shows that EL102 causes loss of cells in G_1, and accumulation of cells in G_2/M within 24 h. This is accompanied by an increase in the number of cells in subG_1 indicating that EL102 has both cytostatic and cytotoxic effects. By 72 h, the majority of cells have entered apoptosis as indicated by accumulation in subG_1, and the decrease in the number of cells in G_2/M. Additionally we again observed a peak beyond G_2/M which represent a subset of cells with increased DNA content (8X), which may represent a subset of cells which advanced through the cell cycle with incomplete cell division.

EL102 inhibits tubulin polymerisation and microtubule formation. The cytotoxic activity of taxanes is exerted by promoting and stabilizing microtubule assembly, while preventing physiological microtubule depolymerisation. To determine the effects of EL102 on taxane induced microtubule assembly, we examined the effects of docetaxel and EL102 on the rate of tubulin polymerisation (Figure 6). As expected docetaxel increased the rate of tubulin polymerisation compared with control untreated tubulin. In contrast, EL102 exhibited a decreased rate of polymerisation compared with control, indicating that EL102 may be an inhibitor of tubulin polymerisation. We also examined the effect of combining EL102 with docetaxel on tubulin polymerisiation rates, which resulted in inhibition of docetaxel induced tubulin polymerisation to levels of inhibition similar to EL102 alone, suggests that these drugs may antagonise each other with respect to their effects on tubulin polymerisation. To connect tubulin polymerisation in a cell-free system to effects on mitosis, we have performed immunofluorescence assays of β-tubulin and acetylated tubulin in DU145 to visualise the microtubules and examine the effects of EL102, docetaxel and combination of both (Figure 7). The data shows an increase in the expression of β-tubulin and acetylated tubulin in response to docetaxel, while EL102 causes a reduction in acetylated tubulin. The combination of EL102 and docetaxel caused a marked change in the distribution of acetylated tubulin becoming increasingly disorganised consistent with a destabilising effect. This coupled with the cell cycle analysis showing loss of cells from G_1 and accumulation in G_2/M at 24 h post treatment (Figure 8) and induction of apoptosis does suggest that microtubule destabilisation is responsible in part for the cytotoxic effects of EL102.

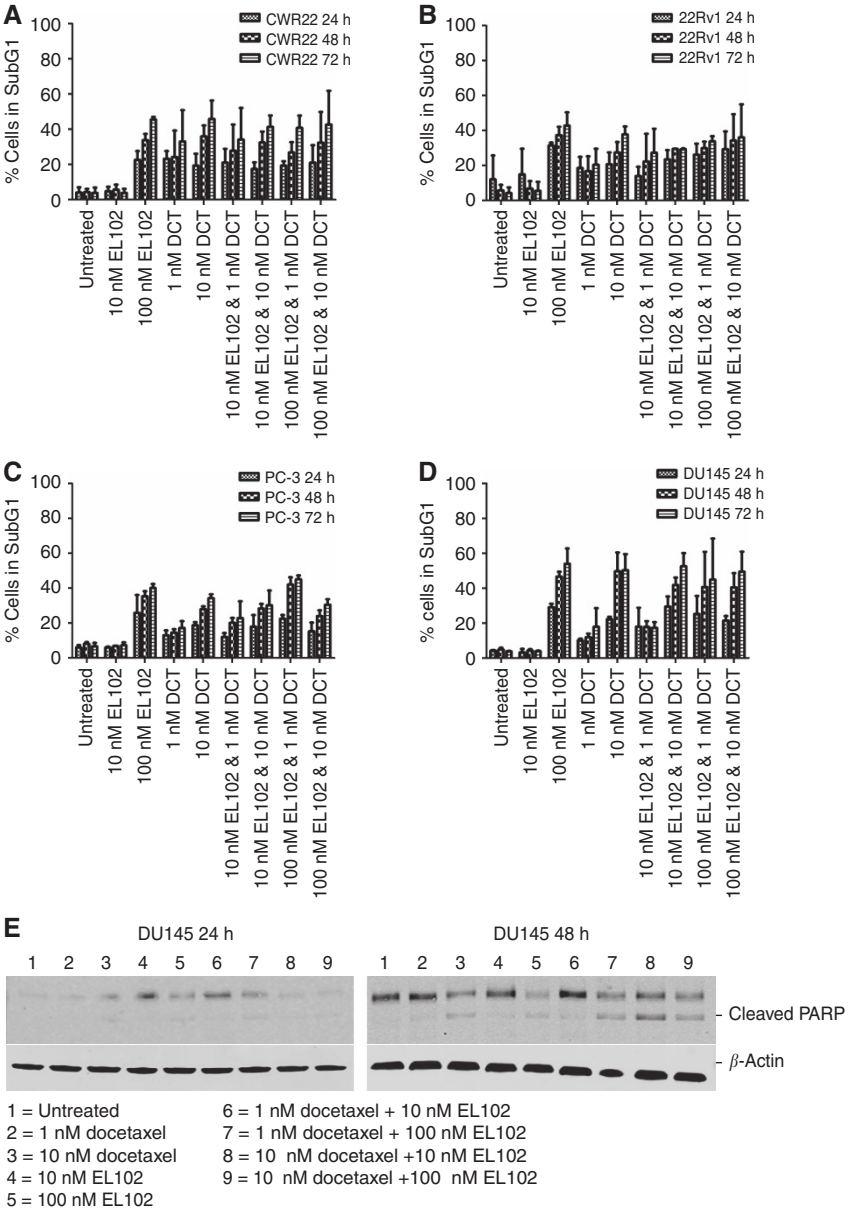

Figure 4. Induction of cellular apoptosis by EL102 and docetaxel. Apoptosis in (**A**) CWR22, (**B**) 22Rv1, (**C**) PC-3 and (**D**) DU145 prostate cancer cell lines as measured by the percentage of cells accumulated in subG$_1$. (See Supplementary Table 4 for results of one-way ANOVA comparing cells in subG$_1$/apoptosis between each treatment). (**E**) PARP cleavage in DU145 protein lysates 24 and 48 h post treatment with EL102 and docetaxel by western blot. Abbreviation: DCT = docetaxel.

EL102 inhibits Hif1α protein expression. EL102 is a later generation derivative of the family of toluidine sulphonamide designed to inhibit Hif1α described by (Wendt *et al*, 2011). We therefore examined the ability of EL102 to inhibit Hif1α in prostate cancer cells (Figure 9). In normoxia, EL102 modestly inhibited Hif1α expression at 50 and 100 nM, but had no effect at 10 nM. We then used cobalt chloride to artificially induce hypoxia-increasing Hif1α expression, and found that EL102 decreased Hif1α at as little as 10 nM.

DISCUSSION

We have established the potential of a novel toluidine sulphonamide EL102 as a potential broad spectrum anti-prostate cancer therapeutic agent. We found that prostate cancer cell lines were sensitive to EL102 at an IC$_{50}$ range of 20–40 nM. Our metastatic prostate cancer cell lines PC-3 and DU145, which are both AR negative and represent castrate-resistant metastatic disease are equally responsive to EL102. The AR-positive cell lines CWR22 and 22Rv1 are twofold more sensitive to EL102 than the metastatic DU145 and PC-3 cell lines.

EL102 is a next-generation derivative of the prototype toluidine sulphonamide compound 1 Hif1 inhibitor (Wendt *et al*, 2011). EL102 was identified as a potential chemotherapeutic agent during a screen of compound 1-derived novel small molecule inhibitors using the NCI-60 cell line panel assessing for growth inhibition potential (not shown). Therefore, we assessed its efficacy for use in the treatment of prostate cancer as a single agent and in combination with the clinically available docetaxel. Docetaxel is a member of the taxane family and is approved for use in prostate cancer patients with castrate-resistant metastatic disease, having been found to provide a modest increase in median survival time

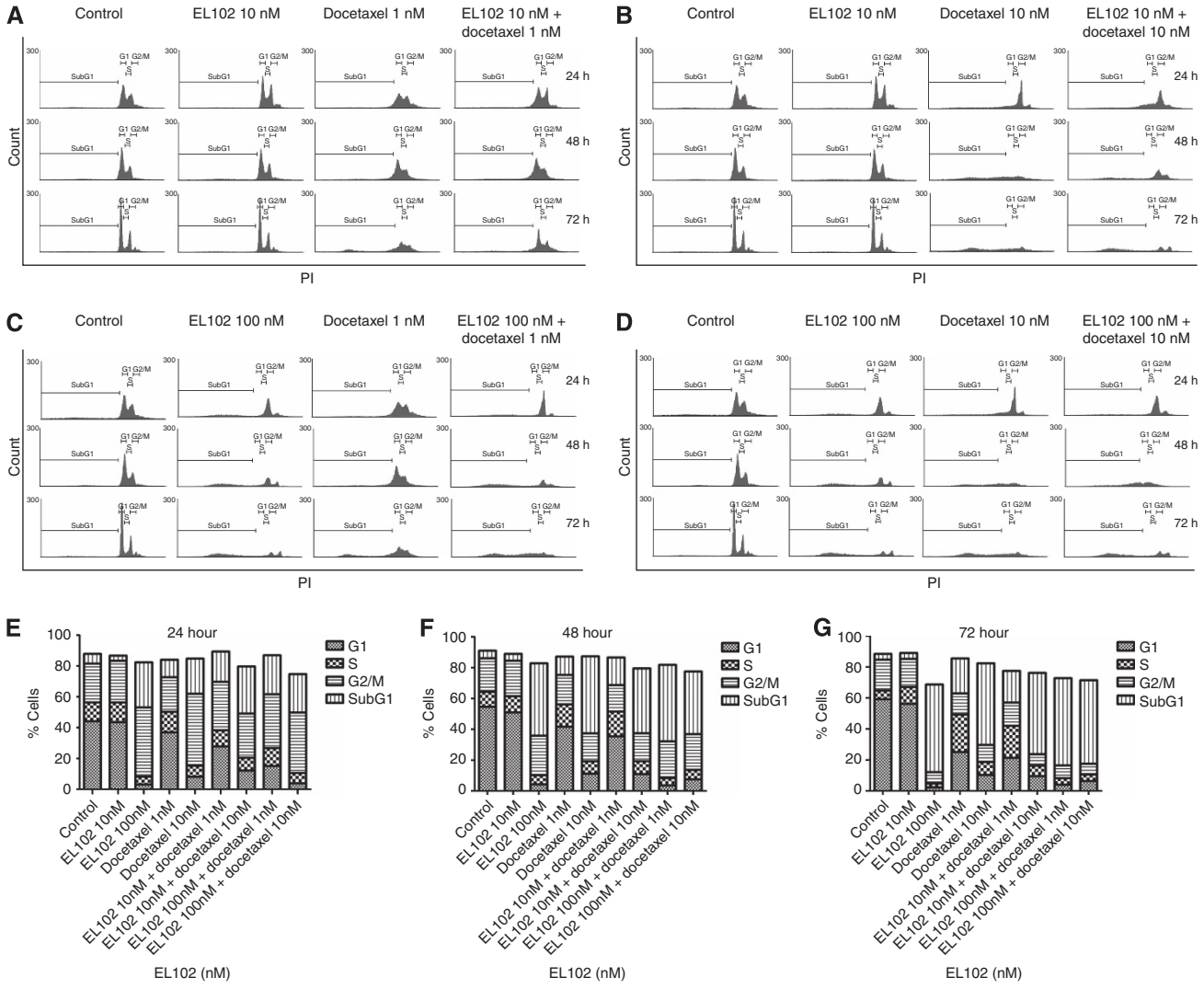

Figure 5. Cell cycle analysis of DU145 cell accumulation in G1, S, G2/M and subG$_1$ after EL102, docetaxel or combination treatment. Cell cycle profiles of DU145 cells, with markers indicating the G1, S, G2/M and subG$_1$ cells, after exposure to (**A**) 10 nM EL102 or 1 nM docetaxel, or 10 nM EL102 and 1 nM docetaxel, (**B**) 10 nM EL102 or 10 nM docetaxel, or 10 nM EL102 and 10 nM docetaxel, (**C**) 100 nM EL102 or 1 nM docetaxel, or 100 nM EL102 and 1 nM docetaxel, (**D**) 100 nM EL102 or 10 nM docetaxel, or 100 nM EL102 and 10 nM docetaxel for 24, 48 and 72 h. Graphs of cell cycle analysis of accumulation of DU145 in the G$_1$, S, G$_2$/M and sub-G$_1$ phase in response to 0, 10 and 100 nM EL102, 1 and 10 nM docetaxel and combinations of each at (**E**) 24, (**F**) 48, (**G**) 72 h as measured by propidium iodide flow cytometry.

when used in combination with prednisone, compared with mitoxantrone and prednisone (19.2 months *vs* 16.3 months median survival) in the TAX327 trial (Berthold *et al*, 2008), and when in combination with extramustine compared with mitoxantrone and prednisone (17.5 months *vs* 15.6 months median survival) in the SWOG9912 trial (Petrylak *et al*, 2004). Until the approval of six new agents in the last 3 years, docetaxel had been the standard of care in the castrate-resistant metastatic setting. Attempts to combine docetaxel with other agents have been largely unsuccessful in terms of efficacy and side-effects (Antonarakis and Eisenberger, 2013).

We observed that EL102 is a cytotoxic agent and also displays cytostatic properties, through flow cytometric analysis of PI-stained cells cultured for 24, 48 and 72 h, following treatment. This was evidenced by the increased number of cells seen in subG$_1$ and G$_2$/M phase of cell cycle, demonstrating that EL102 induces apoptosis and causes G$_2$/M arrest, preventing the cell from entering into mitosis. Further investigation showed that EL102 inhibited tubulin polymerisation and caused destabilisation of the microtubules in DU145 prostate cancer cells. Induction of apoptosis, following 24 and 48 h EL102 treatment was confirmed through western blot analysis of PARP cleavage. Additionally, we found that EL102 decreased Hif1α expression in normoxia and hypoxia *in vitro*, indicating an additional mechanism of action to microtubule destabilisation. Future studies will explore in depth the ability of EL102 to inhibit cell migration and invasion *in vitro* and inhibit a PC-3 xenograft model of bone metastasis, given the role of microtubules in cell polarisation and cell invasion. We will also explore the impact of Hif1α inhibition by EL102 in PC-3 xenograft mouse models and its subsequent effects on the expression of hypoxia-inducible genes, which regulate several key biological processes, including cell proliferation, angiogenesis, metabolism, apoptosis, immortalisation and migration, essential for tumour progression (Harris, 2002).

Several clinical trials have been conducted recently exploring the potential of neoadjuvant chemotherapy in patients with high-risk localised prostate cancer (Womble *et al*, 2011; Narita *et al*, 2012; Ross *et al*, 2012). The results of these trials suggest a benefit to patients in terms of reductions in tumour volume and PSA levels (Womble *et al*, 2011; Ross *et al*, 2012). Given the equal sensitivity

of AR-positive CWR22 and 22Rv1 to EL102 despite their different sensitivity to androgen, this suggests that EL102 could potentially be used in a castrate sensitive setting before the development of hormone resistance. To further investigate this, we postulated that CWR22 cells would respond to EL102 as single agent. This was confirmed in the CWR22 prostate xenograft model.

As mentioned previously attempts to combine docetaxel with other agents have been largely unsuccessful (Antonarakis and Eisenberger, 2013). In this study, our *in vivo* investigations found that the combination of EL102 and docetaxel decreased tumour proliferation of CWR22 xenograft to a great extent than either drug alone. The combination of docetaxel and EL102 significantly decreased tumour growth to a greater extent than either alone in a xenograft model of CWR22. While combining the drugs *in vitro* doesn't have an additive effect on induction of apoptosis, it appears to increase the loss of cells from G_1 and accumulation in G_2/M than either drug alone suggesting the combination may increase cytostatic effects. Additionally combining EL102 and docetaxel, one essentially a tubulin polymerisation destabiliser and the other a tubulin polymerisation stabiliser had an antagonistic effect resulting initially in a slower rate of initial polymerisation followed by inhibition of further polymerisation. Future studies will examine whether EL102's ability to inhibit Hif1α in hypoxic tumours contributes to the observed effects of the combination. Possible downstream effects of Hif1α inhibition include inhibition of angiogenesis and metastasis.

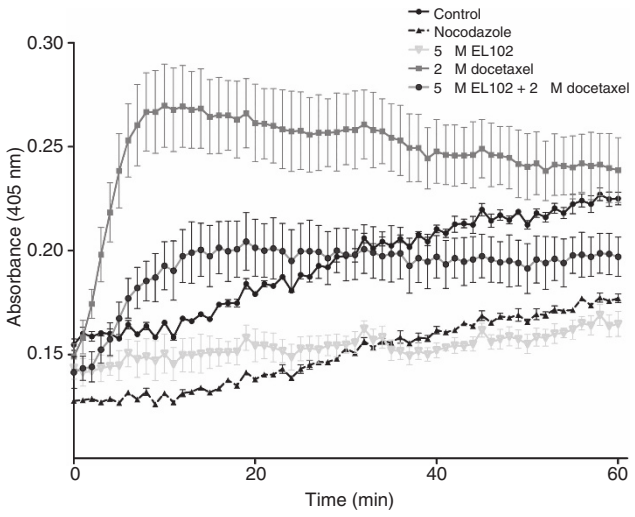

Figure 6. Impact of EL102 and docetaxel alone and in combination on tubulin polymerisation activity. The change in OD ± s.e.m over time (mins) was measured following tubulin's treatment with 5 μM EL102, 2 μM docetaxel and a combination of both *vs* untreated and 2 μM nocodazole.

There is no current cure for castrate-resistant metastatic prostate cancer. Novel adjuvant chemotherapies are continually being developed to address this, with the approval of six new agents since 2010. Recently, clinical trials involving next-generation taxane, cabazitaxel in combination with abiraterone acetate, have begun recruiting patients with preliminary findings expected in 2015. Cabazitaxel is a microtubule-stabilising agent, and is effective in treating patients that have become resistant to docetaxel treatment through overexpression of Pgp (O'Neill *et al*, 2011; Zhang *et al*, 2012), as cabazitaxel is not a substrate for Pgp (Mita *et al*, 2009). Abiraterone functions through disruption of critical steps of androgen formation by direct inhibition of CYP17 activity. This results in reduced levels of circulating androgen and slower progression of prostate cancer in castrate-resistant patients (O'Donnell *et al*, 2004; Agarwal *et al*, 2010). Thus, combining

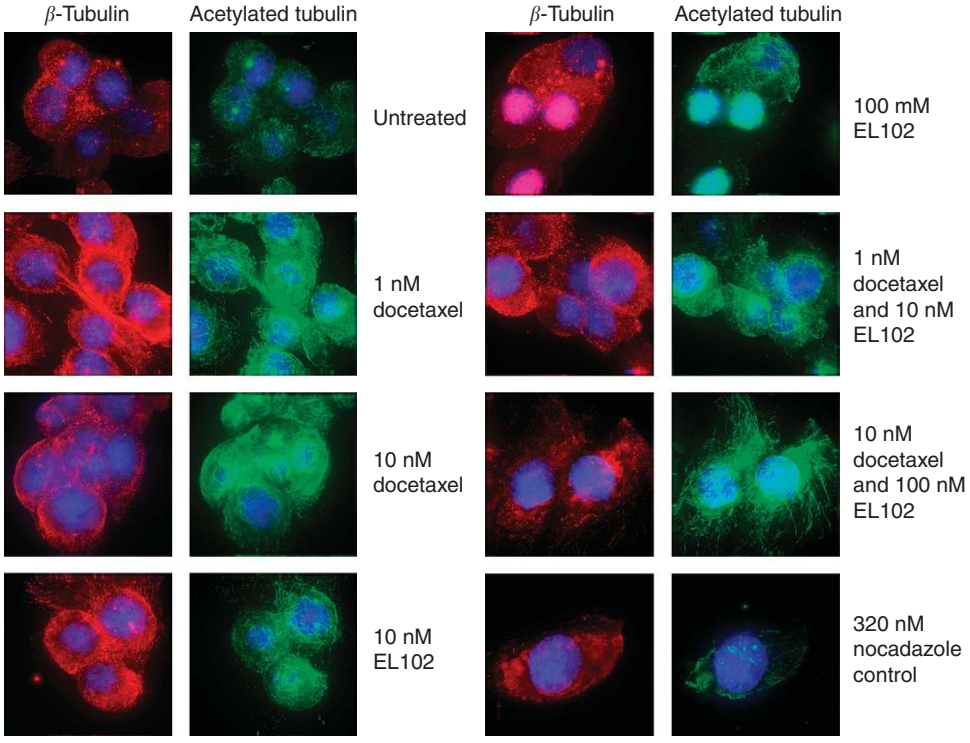

Figure 7. Effect of EL102 on microtubule destabilisation. The effects of EL102 treatments (0, 10, 100 nM), docetaxel treatments (0, 1 and 10 nM) and a combination of both, on microtubule stability in DU145 prostate cancer cells were determined. Following 24 h post-treatment incubation at optimum conditions, cells were fixed with ice-cold methanol and simultaneously stained with Rabbit anti-β-tubulin and anti-acetylated tubulin antibodies. Microtubules were visualised using Alexa Fluor 647 donkey anti-rabbit IgG secondary and Rhodamine Red-X-AffiniPure Fab Fragment goat anti-mouse IgG. Nuclei were counterstained using DAPI.

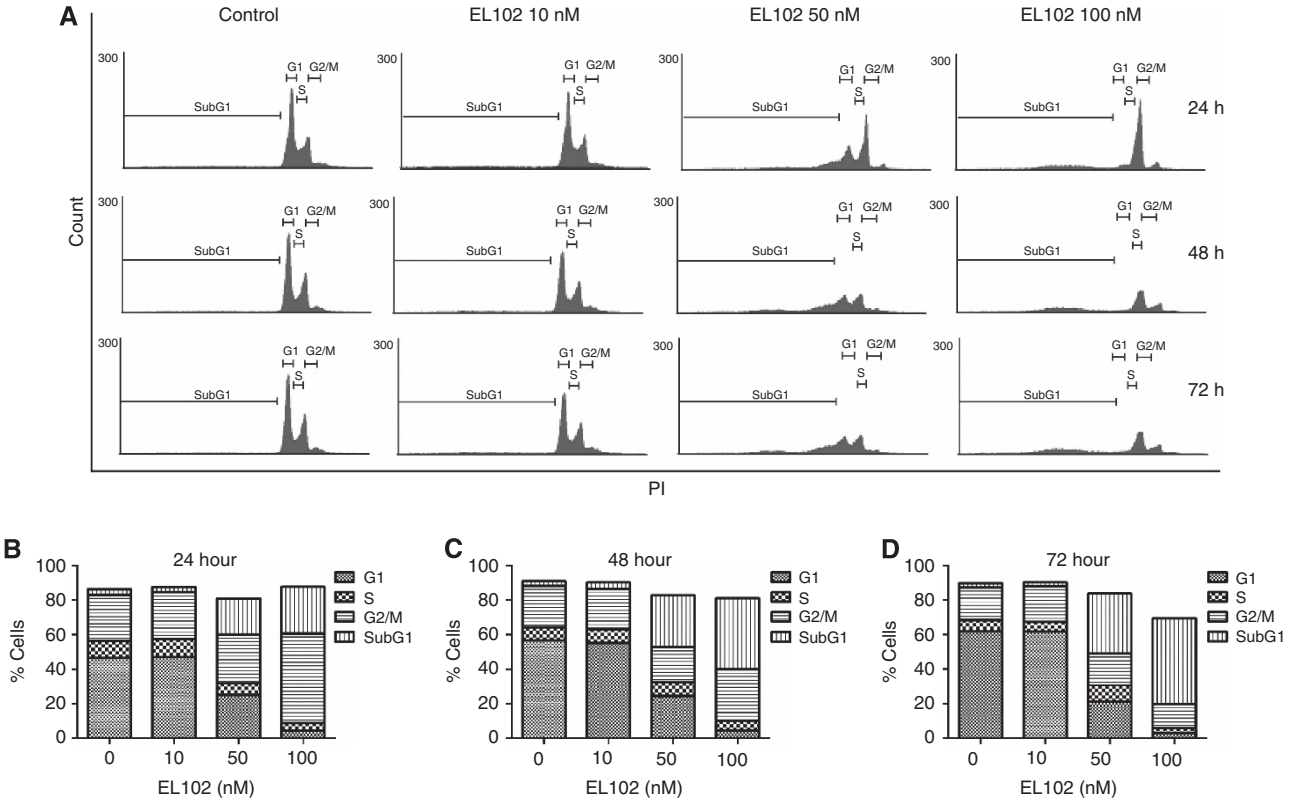

Figure 8. Representative cell cycle analysis of dose response effects of EL102-treated DU145. (**A**) Histograms of cell cycle analysis of accumulation of DU145 in the G_1, S, G_2/M and sub-G_1 phase in response to 0, 10, 50 and 100 nM EL102 at (**B**) 24, (**C**) 48, (**D**) 72 h as measured by linear propidium iodide flow cytometry.

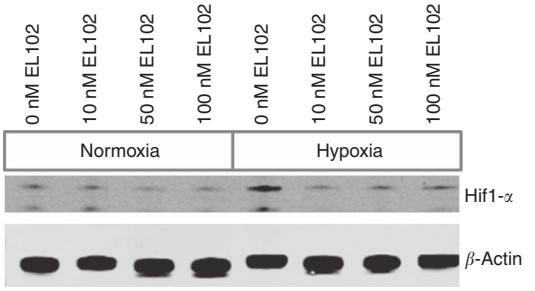

Figure 9. EL102 inhibits Hif1α in normoxia and hypoxia. EL102 inhibited Hif1α in normoxia at 50 and nM. When cells were treated with 100 μm cobalt chloride to induce hypoxia and Hif1α, EL102 was able to inhibit Hif1a stabilisation at 10 nM.

cabazitaxel and abiraterone acetate, allows us to target multiple pathways in mCRPC, while also eliminating Pgp mediated drug resistance. This lends further credence to the argument for introducing novel compounds, such as EL102 which has mechanisms distinct from the mainstay therapies that may work synergistically.

Interestingly, we also found that EL102 overcame Pgp-mediated resistance in the Pgp overexpressing lung cancer cell lines DLKPA, which is cross-resistant to doxorubicin, paclitaxel, docetaxel and vincristine (Clynes *et al*, 1992). While Pgp is an important mechanism of drug resistance in prostate cancer, it is not the only one. Other mechanisms of resistance include altered growth factor receptor pathway activation (e.g., IGFR, VEGFR, EGFR), hypoxia-related resistance, tubulin mutation and altered tubulin isoform expression, and upregulation of other drug pumps in addition to MDR1 (e.g. BCRP, MRP1, MDR2) and NFκB activation (O'Neill *et al*, 2011; Seruga *et al*, 2011; Zhang *et al*, 2012).

In summary, we present data on the efficacy of EL102 as a novel chemotherapeutic agent with potential for the treatment of prostate cancer. We show that EL102 is active in both castration-sensitive and castration-resistant prostate cancer cell lines. EL102 enhances the potency of docetaxel in a xenograft model of the CWR22 prostate cancer. Finally, EL102 is not a substrate for Pgp-mediated drug resistance, indicating that it may be of use in a chemotherapy refractory setting.

ACKNOWLEDGEMENTS

We would like to thank Professor Martin Clynes and Ms Helena Joyce, Dublin City University and Dr Howard Fearnhead and Dr Aideen Ryan, National University of Ireland, Galway, for their advice on this study. We also wish to thank Professor Kevin Sullivan, Emma Harte and Aisling O'Connor for their assistance and expertise in imaging. This work was supported by the Galway University Foundation (RNR1008 to AT, FJS and SAG), the Health Research Board of Ireland Clinical Research Facility, Galway (RSU004 to FJG) and work carried out by EOC in the NCBES High Throughput Screening core facility supported by the PRTLI5 Advancing Medicine through Discovery programme.

REFERENCES

Agarwal N, Hutson TE, Vogelzang NJ, Sonpavde G (2010) Abiraterone acetate: a promising drug for the treatment of castration-resistant prostate cancer. *Future Oncol* **6**(5): 665–679.

Antonarakis ES, Eisenberger MA (2013) Phase III trials with docetaxel-based combinations for metastatic castration-resistant prostate cancer: time to learn from past experiences. *J Clin Oncol* **31**(14): 1709–1712.

Berthold DR, Pond GR, Soban F, de Wit R, Eisenberger M, Tannock IF (2008) Docetaxel plus prednisone or mitoxantrone plus prednisone for advanced prostate cancer: updated survival in the TAX 327 study. *J Clin Oncol* **26**(2): 242–245.

Clynes M, Redmond A, Moran E, Gilvarry U (1992) Multiple drug-resistance in variant of a human non-small cell lung carcinoma cell line, DLKP-A. *Cytotechnology* **10**(1): 75–89.

Collins DM, Crown J, O'Donovan N, Devery A, O'Sullivan F, O'Driscoll L, Clynes M, O'Connor R (2010) Tyrosine kinase inhibitors potentiate the cytotoxicity of MDR-substrate anticancer agents independent of growth factor receptor status in lung cancer cell lines. *Invest New Drugs* **28**(4): 433–444.

Douros J, Suffness M (1981) New natural products under development at the National Cancer Institute. *Recent Results Cancer Res* **76**: 153–175.

Dunne G, Breen L, Collins DM, Roche S, Clynes M, O'Connor R (2011) Modulation of P-gp expression by lapatinib. *Invest New Drugs* **29**(6): 1284–1293.

Ferrero JM, Chamorey E, Oudard S, Dides S, Lesbats G, Cavaglione G, Nouyrigat P, Foa C, Kaphan R (2006) Phase II trial evaluating a docetaxel-capecitabine combination as treatment for hormone-refractory prostate cancer. *Cancer* **107**(4): 738–745.

Garcia JA, Hutson TE, Shepard D, Elson P, Dreicer R (2011) Gemcitabine and docetaxel in metastatic, castrate-resistant prostate cancer: results from a phase 2 trial. *Cancer* **117**(4): 752–757.

German Animal Protection Law and the UICCR (2010) 'Guidelines for the welfare and use of animals in cancer research'. *Brit J Cancer* **102**: 1555–1577.

Harris AL (2002) Hypoxia–a key regulatory factor in tumour growth. *Nat Rev Cancer* **2**(1): 38–47.

Heidegger I, Massoner P, Eder IE, Pircher A, Pichler R, Aigner F, Bektic J, Horninger W, Klocker H (2013) Novel therapeutic approaches for the treatment of castration-resistant prostate cancer. *J Steroid Biochem Mol Biol* **138C**: 248–256.

Jackson JR, Patrick DR, Dar MM, Huang PS (2007) Targeted anti-mitotic therapies: can we improve on tubulin agents? *Nat Rev Cancer* **7**(2): 107–117.

Keenan J, Murphy L, Henry M, Meleady P, Clynes M (2009) Proteomic analysis of multidrug-resistance mechanisms in adriamycin-resistant variants of DLKP, a squamous lung cancer cell line. *Proteomics* **9**(6): 1556–1566.

Kikuno N, Urakami S, Nakamura S, Hiraoka T, Hyuga T, Arichi N, Wake K, Sumura M, Yoneda T, Kishi H, Shigeno K, Shiina H, Igawa M (2007) Phase-II study of docetaxel, estramustine phosphate, and carboplatin in patients with hormone-refractory prostate cancer. *Eur Urol* **51**(5): 1252–1258.

Manfredi JJ, Horwitz SB (1984) Taxol: an antimitotic agent with a new mechanism of action. *Pharmacol Therap* **25**(1): 83–125.

Martin A, Clynes M (1991) Acid phosphatase: endpoint for in vitro toxicity tests. *In Vitro Cell Dev Biol* **27A**(3 Pt 1): 183–184.

Mita AC, Denis LJ, Rowinsky EK, Debono JS, Goetz AD, Ochoa L, Forouzesh B, Beeram M, Patnaik A, Molpus K, Semiond D, Besenval M, Tolcher AW (2009) Phase I and pharmacokinetic study of XRP6258 (RPR 116258A), a novel taxane, administered as a 1-hour infusion every 3 weeks in patients with advanced solid tumors. *Clin Cancer Res* **15**(2): 723–730.

Narita S, Tsuchiya N, Kumazawa T, Maita S, Numakura K, Obara T, Tsuruta H, Saito M, Inoue T, Horikawa Y, Satoh S, Nanjyo H, Habuchi T (2012) Short-term clinicopathological outcome of neoadjuvant chemohormonal therapy comprising complete androgen blockade, followed by treatment with docetaxel and estramustine phosphate before radical prostatectomy in Japanese patients with high-risk localized prostate cancer. *World J Surg Oncol* **10**: 1.

O'Donnell A, Judson I, Dowsett M, Raynaud F, Dearnaley D, Mason M, Harland S, Robbins A, Halbert G, Nutley B, Jarman M (2004) Hormonal impact of the 17alpha-hydroxylase/C(17,20)-lyase inhibitor abiraterone acetate (CB7630) in patients with prostate cancer. *Br J Cancer* **90**(12): 2317–2325.

O'Neill AJ, Prencipe M, Dowling C, Fan Y, Mulrane L, Gallagher WM, O'Connor D, O'Connor R, Devery A, Corcoran C, Rani S, O'Driscoll L, Fitzpatrick JM, Watson RW (2011) Characterisation and manipulation of docetaxel resistant prostate cancer cell lines. *Mol Cancer* **10**: 126.

Oh WK, Halabi S, Kelly WK, Werner C, Godley PA, Vogelzang NJ, Small EJ (2003) A phase II study of estramustine, docetaxel, and carboplatin with granulocyte-colony-stimulating factor support in patients with hormone-refractory prostate carcinoma: Cancer and Leukemia Group B 99813. *Cancer* **98**(12): 2592–2598.

Peinemann F, Grouven U, Hemkens LG, Bartel C, Borchers H, Pinkawa M, Heidenreich A, Sauerland S (2011) Low-dose rate brachytherapy for men with localized prostate cancer. *Cochrane Database Syst Rev* (7): CD008871.

Petrylak DP, Tangen CM, Hussain MH, Lara Jr. PN, Jones JA, Taplin ME, Burch PA, Berry D, Moinpour C, Kohli M, Benson MC, Small EJ, Raghavan D, Crawford ED (2004) Docetaxel and estramustine compared with mitoxantrone and prednisone for advanced refractory prostate cancer. *N Engl J Med* **351**(15): 1513–1520.

Ross RW, Galsky MD, Febbo P, Barry M, Richie JP, Xie W, Fennessy FM, Bhatt RS, Hayes J, Choueiri TK, Tempany CM, Kantoff PW, Taplin ME, Oh WK (2012) Phase 2 study of neoadjuvant docetaxel plus bevacizumab in patients with high-risk localized prostate cancer: a Prostate Cancer Clinical Trials Consortium trial. *Cancer* **118**(19): 4777–4784.

Rowinsky EK, Cazenave LA, Donehower RC (1990) Taxol: a novel investigational antimicrotubule agent. *J Natl Cancer Inst* **82**(15): 1247–1259.

Seruga B, Ocana A, Tannock IF (2011) Drug resistance in metastatic castration-resistant prostate cancer. *Nat Rev Clin Oncol* **8**(1): 12–23.

Tester W, Ackler J, Tijani L, Leighton J (2006) Phase I/II study of weekly docetaxel and vinblastine in the treatment of metastatic hormone-refractory prostate carcinoma. *Cancer J* **12**(4): 299–304.

Vichai V, Kirtikara K (2006) Sulforhodamine B colorimetric assay for cytotoxicity screening. *Nat Protoc* **1**(3): 1112–1116.

Wani MC, Taylor HL, Wall ME, Coggon P, McPhail AT (1971) Plant antitumor agents. VI. The isolation and structure of taxol, a novel antileukemic and antitumor agent from Taxus brevifolia. *J Am Chem Soc* **93**(9): 2325–2327.

Wendt B, Mulbaier M, Wawro S, Schultes C, Alonso J, Janssen B, Lewis J (2011) Toluidinesulfonamide hypoxia-induced factor 1 inhibitors: alleviating drug-drug interactions through use of PubChem data and comparative molecular field analysis guided synthesis. *J Med Chem* **54**(11): 3982–3986.

Womble PR, VanVeldhuizen PJ, Nisbet AA, Reed GA, Thrasher JB, Holzbeierlein JM (2011) A phase II clinical trial of neoadjuvant ketoconazole and docetaxel chemotherapy before radical prostatectomy in high risk patients. *J Urol* **186**(3): 882–887.

Zhang B, Suer S, Livak F, Adediran S, Vemula A, Khan MA, Ning Y, Hussain A (2012) Telomere and microtubule targeting in treatment-sensitive and treatment-resistant human prostate cancer cells. *Mol Pharmacol* **82**(2): 310–321.

Supplementary Information accompanies this paper on British Journal of Cancer website (http://www.nature.com/bjc)